"One-pot" aminolysis/thia-Michael addition preparation of well-defined amphiphilic PVDF-b-PEG-b-PVDF triblock copolymers: self-assembly behaviour in mixed solvents

Enrique Folgado, Marc Guerre, Antonio Da Costa, Anthony Ferri, Ahmed Addad, Vincent Ladmiral, M. Semsarilar

HAL Id: hal-02462556

https://hal.umontpellier.fr/hal-02462556

Submitted on 15 Nov 2020

Journal Name

ARTICLE

"One-Pot" Aminolysis/Thia-Michael Addition preparation of well-defined amphiphilic PVDF-*b*-PEG-*b*-PVDF triblock copolymers: Self-assembly behaviour in mixed solvents

Enrique Folgado,[a,b] Marc Guerre,[a†] Antonio Da Costa,[c] Anthony Ferri,[c] Ahmed Addad,[d] Vincent Ladmiral,[a]* and Mona Semsarilar[b]*

Polyvinylidene fluoride- (PVDF) containing block copolymers are scarce and difficult to prepare. Amphiphilic block copolymers containing PVDF have been rarely reported. In consequence, few studies of the self-assembly of PVDF-based block copolymers exist. Here a new synthetic route to prepare poly(vinylidene fluoride)-block-poly(ethylene glycol)-block-poly(vinylidene fluoride) (PVDF-*b*-PEG-*b*-PVDF) ABA triblock copolymer is presented. The synthesis relies on the efficient coupling of a PVDF prepared by RAFT and a PEG diacrylate in one pot via aminolysis of the xanthate moiety and subsequent thia-Michael addition. The novel amphiphilic triblock copolymer was fully characterized by ^{1}H and ^{19}F NMR spectroscopies, GPC, TGA, DSC and XRD; and its self-assembly in water and ethanol was studied. Micellization (addition of a selective solvent for PVDF to a solution of the triblock) and nanoprecipitation (addition of a solution of the triblock into a non solvent of PVDF) protocols led to the formation of micelles and vesicles. Surprisingly, under nanoprecipitation conditions (in THF/ ethanol), well-defined crystalline micrometric structures were obtained.

Introduction

ABA triblock copolymers are important materials which have found high added value applications. SBS (polystyrene-*b*-polybutadiene-*b*-polystyrene) are crucial thermoplastic elastomers for the tyre industry for example, and Pluronics® are used in numerous fields as dispersants, emulsifiers, thickeners, antifoaming or wetting agent.[1,2]

Amphiphilic ABA triblock copolymers are indeed very interesting polymer architectures. When the A and B blocks are incompatible, these triblock copolymers readily self-assemble from the melt into well-ordered nanostructures.[3–6] In selective solvents, the self-assembly of such ABA triblock copolymers can generate a variety of morphologies, such as spherical micelles,[7] wormlike micelles,[8] vesicles[9] or more

complex structures such as toroids.[10] In aqueous media, and when the B block is hydrophilic, these triblocks readily form self-assembled micelles comprising a hydrophobic core constituted of the A segments, and a stabilizing hydrophilic corona made of the hydrophilic B blocks.[9,11,12] These micelles, sometimes named flower-like micelles,[4,7] may connect to each other via intermicellar bridges. The formation of these bridges depends on several factors such as micelle concentration, size and nature of A and B blocks and interchain interactions for example.[13,14]

The formation of such bridges is favoured when the hydrophobic core-forming block is smaller than the stabilizing corona segments.[15,16] If the hydrophilic block is too short, the conformational energy will not be favourable to the formation of loops. There must be a compromise between inter-chain interactions, increasing with the length of the hydrophilic block, and the formation of loops, also favored by longer chains. Finally, if the system is too diluted, the intermicellar interactions will be too rare for bridges to form.[17]

In industry most ABA triblock copolymers are prepared by anionic polymerization.[12,18] However, progress in Reversible Deactivation Radical Polymerization (RDRP) techniques, such as RAFT (Reversible Addition-Fragmentation chain Transfer),[19,20] ATRP (Atom-Transfer Radical Polymerization)[21,22] or CMRP (Cobalt-Mediated Radical Polymerization)[23] for example, have enabled the facile synthesis of ABA triblock copolymers. Numerous acrylates-, methacrylates- or styrenics-based ABA triblock copolymers have been described and

[a]Institut Charles Gerhardt Montpellier, ICGM UMR5253, Univ Montpellier, CNRS, ENSCM, Montpellier, France.
[b]Institut Européen des Membranes, IEM, UMR5635, Univ Montpellier, CNRS, ENSCM, Montpellier, France.
[c]Université Artois, CNRS, Centrale Lille, ENSCL, Université Lille, UMR 8181, Unité de Catalyse et Chimie du Solide (UCCS), F-62300 Lens, France.
[d]Université Lille, Sciences et Technologies, CNRS, Unité Matériaux Et Transformations (UMET), F-59000 Lille, France

†Current address : Department of Organic and Macromolecular Chemistry, Centre of Macromolecular Chemistry, Polymer Chemistry Research Group and Laboratory for Organic Synthesis, Ghent University, Krijgslaan 281 S4-bis , B-9000, Ghent, Belgium.

reported by academic research groups. Singha et al. reported the use of ATRP for the preparation of an ABA PDCPMA-*b*-PHEA-*b*-PDCPMA (DCPMA = dicyclopentyloxyethyl methacrylate, EHA = 2-ethylhexylacrylate) triblock copolymer using a Br-PEHA-Br difunctional macroinitiator.[24] Xie et al. synthesised via activator generated by electron transfer (AGET) ATRP, a poly(n-butylacrylate) homopolymer and a polystyrene-*b*-poly(n-butylacrylate)-*b*-polystyrene (PS-PnBA-PS) triblock copolymer from ethylene bis(2-bromoisobutyrate).[25] Following a similar approach and using a difunctional trithiocarbonate RAFT agent, Semsarilar et al. synthesised a polystyrene-*b*-poly(sodium 4-styrenesulfonate)-*b*-polystyrene (PS-*b*-PNaSS-*b*-PS) ABA triblock.[9] Shipp et al. employed a difunctional polydimethylsiloxane xanthate macro RAFT agents to polymerize *N*-vinylpyrrolidone (NVP) and prepare a PVP-*b*-PDMS-*b*-PVP ABA triblock copolymer.[26] CMRP is particularly well-adapted to prepare ABA triblock copolymers from LAMs (less-activated monomers) such as vinyl acetate for example.[27] It is arguably the most efficient method to control the polymerization of LAMs and to prepare well-defined copolymers from these type of monomers.[27] ABA triblock copolymers are also very easily synthesized by CMRP from diblock copolymers using a very efficient radical coupling cobalt-catalyzed chemistry.[23,28–31]

Fluorinated polymers bearing fluorine atoms on the main chain such as PTFE (polytetrafluoroethylene) or PVDF (poly(vinylidene fluoride)) are valuable specialty polymers endowed with remarkable properties. PVDF in particular displays high resistance to weathering and chemical aggressions as well as unusual electroactivity. Copolymers of VDF, trifluoroethylene and chlorotrifluoroethylene for example are outstanding relaxor ferroelectrics. [32–34,]Copolymers of VDF and TrFE possess high sensitivity and wide frequency responses to electric fields, are relatively flexible, and easy to produce. These copolymers have a great potential for emerging applications such as haptics, sensors, artificial muscles, etc.[35]

Only few references describe the self-assembly of PVDF block copolymers in solution, probably because well-defined PVDF-containing block copolymers are difficult to synthesize.[36–38] Qian et al. studied the self-assembly of PVDF-*b*-PS block copolymers in DMF-containing mixtures of solvents. The presence of DMF was necessary to give sufficient mobility to the PVDF segments and gain access to non-spherical self-assembled structures.[39] Rodionov et al. prepared interesting 4-miktoarm star copolymers containing 2 PVDF-*b*-PS arms and 2 PEG arms via the combination of ATRP, Iodine Transfer Polymerization (ITP) and copper-catalyzed azide-alkyne cycloaddition (CuAAC); and studied their self-assembly in organic solvents and water.[40] Over the last two years we developed the RAFT polymerization of VDF,[41] and prepared some PVDF-containing block copolymers,[42] which self-assembled in water and organic solvents. PVDF-*b*-PVA (PVA = poly(vinyl alcohol)) formed spherical particles in water,[43]

PVDF-*b*-PDMAEMA (PDMAEMA = poly (2-dimethylaminoethyl methacrylate) in water displayed spherical aggregates and rigid rods which are thought to be generated via crystallisation-driven self-assembly;[44] and PVAc-*b*-PVDF (PVAc = poly(vinyl acetate)) readily self-assembled in dimethyl carbonate under polymerization-induced self-assembly conditions into highly crystalline micrometric structures.[45] The synthesis of PVDF-based BCPs by RAFT (or ITP) and sequential addition of monomers is difficult due to the fast accumulation of much less reactive inversely-terminated PVDF chains (-CH₂-xanthate-terminated chains). For example, in spite of what was recently wrongly reported,[46] well-defined PVDF-*b*-PNVP (PNVP = poly *N*-vinyl pyrrolidone) cannot be synthesized by polymerization of NVP starting from a PVDF macroRAFT agent since only -CF₂-xanthate-terminated chains (which disappear entirely from the reaction medium quickly) can be reinitiated with PNVP radicals.[37] Synthesis strategies based on the coupling of two or more homopolymers may afford better-defined block copolymers provided the coupling reaction is efficient enough, although complete removal of the residual homopolymers is often difficult or requires tedious purification steps. Huck et al., for example, purified a PF8TBT-*b*-P3HT diblock copolymer (P3HT = poly(3-hexylthiophene) and PF8TBT = poly((9,9-dioctylfluorene)-2,7-diyl-alt-[4,7-bis(3hexylthien-5-yl)-2,1,3-benzothiadiazole]-2',2''-diyl)) via preparative GPC to remove the excess of P3HT homopolymer.[47] This strategy has been successfully implemented with the copper-catalyzed coupling of azides and alkynes (CuAAC) to prepare PVDF-block copolymers[45] and PEG-*b*-PFPE-*b*-PEG (PEG = polyethylene glycol, PFPE = perfluoropolyether) ABA triblock copolymers.[7] CuAAC is a powerful click chemistry technique, but the removal of copper is often tedious. In contrast, the thia-Michael addition does not use copper, and is very well-suited to polymers made by RAFT.[48,49] It does not require functional RAFT agents and can be conducted in one pot.[50,51]

In this paper, we report the synthesis using RAFT polymerization and a one-pot thia-Michael addition procedure, the characterization of a novel amphiphilic PVDF-based ABA triblock copolymer (PVDF₅₀-*b*-PEG₁₃₆-*b*-PVDF₅₀), its self-assembly in NMP/water, THF/ethanol and THF/water mixtures and the characterization of the obtained structures using TEM and AFM.

Experimental section

Materials

All reagents were used as received unless otherwise stated. 1,1-Difluoroethylene (vinylidene fluoride, VDF) was supplied by Arkema (Pierre-Bénite, France). *O*-Ethyl-*S*-(1-methoxycarbonyl) ethyldithiocarbonate was synthesized according to the method described by Liu et al.[52] *Tert*-Amyl peroxy-2-ethylhexanoate (Trigonox 121, purity 95%) was purchased from AkzoNobel (Chalons-sur-Marne, France). PEG₆₀₀₀, acetonitrile (ACN),

ethanol (EtOH), dimethyl carbonate (DMC), hexylamine, *N*-methyl-2-pyrrolidone (NMP), tetrahydrofuran (THF), triethylamine (NEt₃) and laboratory reagent grade hexane (purity >95%) were purchased from Sigma-Aldrich.

Measurements

Nuclear Magnetic Resonance (NMR) The NMR spectra were recorded on a Bruker AV III HD Spectrometer (400 MHz for ^{1}H and 376 MHz for ^{19}F).

Coupling constants and chemical shifts are given in hertz (Hz) and parts per million (ppm), respectively. The experimental conditions for recording ^{1}H and ^{19}F NMR spectra were as follows: flip angle, 90° (or 30°); acquisition time, 4.5 s (or 2 s); pulse delay, 2 s; number of scans, 32 (or 64); and pulse widths of 12.5 and 11.4 µs for ^{1}H and ^{19}F NMR respectively. 2D DOSY (Diffusion-Ordered Spectroscopy) NMR spectra were recorded at 60 °C on a Bruker Avance 300 MHz spectrometer using deuterated DMSO. All experiments were recorded in static mode (spinning off) with a Bruker Dual z-gradient probe producing gradients in the z direction with strength 55 G cm^{-1}. DOSY proton spectra were acquired with pulsed-gradient stimulated echo (LED-PFGSTE) sequence, using a bipolar gradient. All spectra were recorded with 8 Ko time domain data points in the F2 Frequency axis and 32 experiments (F1). The gradient strength was logarithmically incremented in 32 steps from 2% up to 95% of the maximum gradient strength. All measurements were performed with a diffusion delay (D) of 50 ms in order to keep the relaxation contribution to the signal attenuation constant for all samples. The gradient pulse length (δ) was 3.5 ms in order to ensure full signal attenuation. The diffusion dimension of the 2D DOSY spectra was processed according to the TopSpin standard conditions (version 2.1).

Size-Exclusion Chromatography (SEC). SEC measurements were recorded using a triple-detection GPC from Agilent Technologies with its corresponding Agilent software, dedicated to multidetector GPC calculation. The system used two PL1113-6300 ResiPore 300 × 7.5 mm columns with THF the eluent with a flow rate of 0.8 mL·min^{-1} and toluene as the flow rate marker. The detector suite was composed of a PL0390-0605390 LC light scattering detector with two diffusion angles (15° and 90°), a PL0390-06034 capillary viscometer, and a 390-LC PL0390-0601 refractive index detector. The entire SEC-HPLC system was thermostated at 35 °C. PMMA standards were used for calibration. Typical sample concentration was 10 mg/mL.

Differential Scanning Calorimetry (DSC). DSC measurements were performed on 2–3 mg samples on a TA Instruments DSC Q20 equipped with an RCS90 cooling system. For all measurements, the following heating / cooling cycle was employed: cooling from room temperature (ca. 20 °C) to −73 °C at 20 °C/min, isotherm plateau at −50 °C for 5 min, first heating ramp from −73 °C to 250 °C at 10 °C/min, cooling stage from 250 °C to −73 °C at 10 °C/min, isotherm plateau at −73 °C

for 3 min, second heating ramp from −73 °C to 250 °C at 10 °C/min, and last cooling stage from 250 °C to room temperature (ca. 20 °C). Calibration of the instrument was performed with noble metals and checked before analysis with an indium sample. Melting points were determined at the maximum of the enthalpy peaks.

Thermogravimetric analysis (TGA). TGA analyses were carried out with a TA Instruments TGA G500 from 20 °C to 1000 °C. A heating rate of 10 °C min^{-1} was used under an air atmosphere with a flow rate of 60 mL min^{-1}. A dry sample weighing about 3 mg was used.

Dynamic light scattering (DLS). DLS measurements of polymer solutions in NMP and THF were carried out in a Malvern ZEN1600 using a quartz cuvette.

Transmission electron microscopy (TEM). TEM studies were conducted using a JEOL 1200 EXII instrument equipped with a numerical camera, operating with a 120 kV acceleration voltage at 25 °C. To prepare TEM samples, a drop (7.0 µL) of a dilute micellar solution was placed onto a carbon-coated copper grid for 50 s, blotted with filter paper and dried under ambient conditions.
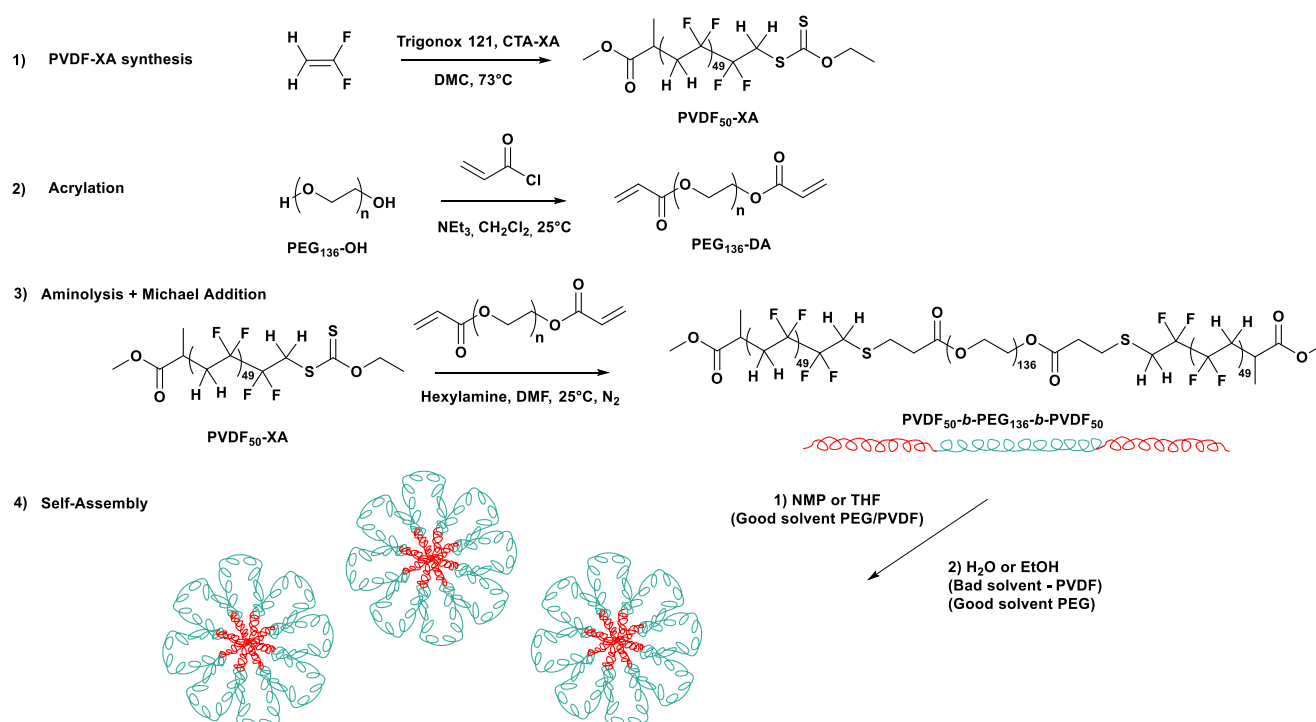
Atomic force microscopy (AFM). AFM images were obtained with a Pico SPM II provided by Molecular Imaging. The imagery was controlled by the PicoView 1.10 software. The experiments were all carried out in tapping mode. The types of tips used were PPS-FMR purchased from Nanosensors with a frequency resonance between 45 and 115 kHz and a force constant between 0.5 and 9.5 N/m. Gwyddion 2.25 software was used to treat the images.

X-Ray diffraction (XRD). XRD powder patterns were carried out on a Philips X'pert Pro MPD diffractometer by using Ni-filtered CuKα1 radiation (λ=1.5406 Å) in Bragg–Brentano scanning mode with a 2θ angle range from 5–60°, and a time per step of 50 s.

Synthesis

Autoclave. The polymerization of VDF was performed in a 100 mL Hastelloy Parr autoclave system (HC 276) equipped with a mechanical Hastelloy stirring system, a rupture disk (3000 PSI), inlet and outlet valves, and a Parr electronic controller to regulate the stirring speed and heating.

PVDF₅₀-XA synthesis A solution of Trigonox 121 (158 mg, 6.87 10^{-4} mol) and *O*-Ethyl-*S*-(1-methoxycarbonyl) ethyldithiocarbonate (1.30 g, 6.25 10^{-3} mol) in DMC (60 mL), was degassed by N₂ bubbling during 30 min. Prior to the reaction, the autoclave was pressurized with 30 bar of nitrogen to check for leaks. The autoclave was then put under vacuum (20 10^{-3} mbar) for 30 min to remove any trace of oxygen. The homogenous DMC solution was introduced into the autoclave using a funnel, VDF gas (19.0 g, 2.97 10^{-1} mol) was transferred in the autoclave at low temperature, and the reactor was gradually heated to 73 °C. The reaction was stopped after 18 h. The autoclave was cooled down to room

Journal Name

ARTICLE

Scheme 1. Synthesis and self-assembly of the amphiphilic PVDF-*b*-PEG-*b*-PVDF ABA triblock copolymer. 1) Synthesis of PVDF-XA by RAFT. 2) PEG diacrylate (PEGDA) synthesis in dichloromethane using acryloyl chloride. 3) One-pot synthesis of the triblock copolymer by aminolysis of the xanthate groups and thia-Michael addition of the resulting PVDF-SH to PEGDA. 4) Self-assembly into expected flower-like micelles of the ABA triblock copolymer (nanoprecipitation or micellization).

temperature (ca. 20 °C), purged from the residual monomers, and DMC was removed under vacuum. The crude product was dissolved in 30 mL of warm THF (ca. 40 °C), and left under vigorous stirring for 30 minutes. This polymer solution was then precipitated from 400 mL of chilled hexane. The precipitated polymer (white powder) was filtered through a filter funnel and dried under vacuum ($15 \cdot 10^{-3}$ mbar) for two hours at 50°C. The polymerization yield (65%) was determined gravimetrically (mass of dried precipitated polymers / mass of monomer introduced in the pressure reactor).

^{1}H NMR (400 MHz (CD$_3$)$_2$CO, δ (ppm), Figure S1): 1.09 (d, -CH(C**H$_3$**)(C=O)-, $^3J_{HH}$ = 7.1 Hz), 1.31 (t, -S(C=S)-O-CH$_2$-C**H$_3$**, $^3J_{HH}$ = 7.1 Hz), 2.13-2.31 (m,-CF$_2$-C**H$_2$**-C**H$_2$**-CF$_2$-, VDF-VDF TT reverse addition), 2.66-3.01 (t, -CF$_2$-C**H$_2$**-CF$_2$-, VDF-VDF HT regular addition), 3.48–3.57 (s, -(C=O)-O-C**H$_3$**), 3.97 (t, -CF$_2$-C**H$_2$**-S(C=S)OEt, $^3J_{HF}$ = 17.7 Hz), 4.59 (q, (-S(C=S)OC**H$_2$**-CH$_3$, $^3J_{HH}$ = 7.0 Hz), 6.05-6.45 (tt, $^2J_{HF}$ = 55 Hz , $^3J_{HH}$ = 4.6 Hz -CH$_2$-CF$_2$-**H**).

^{19}F NMR (376 MHz (CD$_3$)$_2$CO, δ (ppm), Figure S2): -115.64 (-CH$_2$-CF$_2$-C**F$_2$**-CH$_2$-CH$_2$-, VDF-VDF HH reverse addition), -114.29 ($^2J_{HF}$ = 55 Hz, -CH$_2$-C**F$_2$**-H), -113.35 (-CH$_2$-C**F$_2$**-CF$_2$-CH$_2$-CH$_2$-, HH reverse addition), -113.09 (CH$_2$-CF$_2$-C**F$_2$**-CH$_2$-S-), -112.69 (-CH$_2$-

C**F$_2$**-CF$_2$-CH$_2$-S-), -94.79 (-CH$_2$-CH$_2$-C**F$_2$**-CH$_2$-, TT reverse addition), -93.50 (-CH$_2$-C**F$_2$**-CH$_2$-CH(CH$_3$)(C=O)-), -92.12 (-CH$_2$-C**F$_2$**-CH$_2$-CF$_2$H), -91.43 (-CH$_2$-CH$_2$-CF$_2$-CH$_2$-C**F$_2$**-CH$_2$-CF$_2$-, regular VDF-VDF HT addition), -91.00 (-CH$_2$-C**F$_2$**-CH$_2$-, regular VDF-VDF HT addition).

The degree of polymerization (DP) and number average molar mass of PVDF were calculated from the ^{1}H NMR spectrum using the following equations:

$$DP = \frac{\int_{2.66}^{3.01} CH_2(HT) + \int_{2.13}^{2.31} CH_2(TT) + \int_{3.89}^{4.06} CH_2(End-group)}{2/3 \times \int_{1.03}^{1.14} CH_3 (R-CTA_{XA})}$$

$$M_{n,NMR}(R) = M_{n,CTA} + (DP \times M_{n,VDF})$$

Where $M_{n\,CTA}$ = 208.3 g.mol^{-1} and $M_{n\,VDF}$ = 64.04 g.mol^{-1}

According to these equations, DP = 50, and $M_{n,NMR}$ = 3400 g.mol^{-1}

PEGDA$_{136}$ synthesis. PEG diacrylates were obtained from commercial PEG$_{6000}$ as follows: polyethylene glycol (PEG$_{6000}$; 7 g; 1.17 mmol; 1 eq.) and acryloyl chloride (0.95 mL; 11.7 mmol; 10 eq.) were dissolved in dichloromethane (DCM, 48 mL) in a

round bottom flask under magnetic stirring at room temperature (25°C). After 10 min, triethylamine (TEA, 0.47 g, 4.68 mmol, 4 eq) was added dropwise The reaction was monitored by ^{1}H NMR. After 60h, the precipitate was filtered off on Celite, and the target polymer was precipitated in cold diethyl ether and then dried under vacuum.

^{1}H NMR (400 MHz, $(CD_3)_2SO$) δ (ppm), Figure S4): 6.43 (d, J=17.3 Hz, 2H, -CH=C**H$_2$**), 6.16 (dd, J=17.4 Hz and 10.4 Hz, 2H, -C=C**H**-C=O), 5.85 (d, J= 10.4 Hz, 2H, -CH=C**H$_2$**), 4.23 (m, 2H, -(C=O)-O-C**H$_2$**-CH$_2$-O-) 3.4-3.8 (m, -C**H$_2$**-C**H$_2$**-O).

PVDF-*b*-PEG-*b*-PVDF triblock synthesis. PVDF$_{50}$-XA (5.000 g, 1.47 mmol) and PEGDA$_{136}$ (4.410 g, 0.735 mmol) were dissolved in DMF (115 mL). The mixture was degassed with N$_2$ (10 min). A degassed mixture of hexylamine (0.612 g, 6.05 mmol) and triethylamine (TEA, 2.15 mmol) in DMF was injected into the reaction mixture. N$_2$ was bubbled for another 10 min. The mixture was stirred 16 h until the reaction was complete and no unreacted acrylate could be detected by ^{1}H NMR. The product was then precipitated twice in cold diethyl ether.

^{1}H NMR (400 MHz $(CD_3)_2SO$, δ (ppm), Figure S5) : 1.15-1,20 - CH(C**H$_3$**)(C=O)-, 2.16-2.38 (m, -CF$_2$-C**H$_2$**-C**H$_2$**-CF$_2$-, VDF-VDF TT reverse addition), 2.62-2.71 (m, -S-CH$_2$-C**H$_2$**(C=O)), 2.71-3.05 (t, -CF$_2$-C**H$_2$**-CF$_2$-, VDF-VDF HT regular addition), 3.07-3.14 (m, CF$_2$-CF$_2$-C**H$_2$**-S), 3.42-3.60 (m, -(O-(C**H$_2$**-C**H$_2$**)), 3.60-3.69 (s, -(C=O)-O-C**H$_3$**), 3.72-3.81 (m, -C(C=O)-O-CH$_2$-C**H$_2$**) 4.13-4.23 (-C(C=O)-O-CH$_2$-C**H$_2$**). ^{19}F NMR (377 MHz, $(CD_3)_2SO$ δ (ppm), Figure S6): -115.16 (-CH$_2$-CF$_2$-C**F$_2$**-CH$_2$-CH$_2$-), -113.77(-CH$_2$-C**F$_2$**-CF$_2$-CH$_2$-CH$_2$-), -112.87 (-CH-CF$_2$-C**F$_2$**-CH$_2$-S-), -112.25 (-CH$_2$-C**F$_2$**-CF$_2$-CH$_2$-S-), -93.75 (-CH$_2$-CH$_2$-C**F$_2$**-CH$_2$-CF$_2$-), -92.76 (CH$_3$-O-(C=O)-(CH$_3$)C$_H$-CH$_2$-C**F$_2$**-), -91.82 (-CH$_2$-C**F$_2$**-CH$_2$-CF$_2$-H), -91.46 (-CH$_2$-CH$_2$-CF$_2$-CH$_2$-C**F$_2$**-CH$_2$-CF$_2$), -91.00 (-CH$_2$-C**F$_2$**-CH$_2$-, regular VDF-VDF HT addition).

Self-assembly

Preparation of the solution

A 5% w/w triblock copolymer solution in NMP (60 mg of triblock copolymer in 1.2 mL of solvent) and another solution in THF at 1% w/w (24 mg of triblock copolymer in 2.4 mL of solvent) were prepared in glass vials and heated to 70 °C in the case of NMP and to 60 °C in the case of THF for at least 24h.

Micellization protocol

To different glass vials placed in a stirring plate and equipped with magnetic bars were added 0.2 mL of triblock solution (5% w/w in NMP or 1% w/w in THF). To each vial a non-solvent for PVDF was added dropwise to reach different solvent/non-solvent ratios (i.e. 0.4 mL for 1:2 ratio; 0.8 mL for 1:4 ratio; 1.2 mL for 1:6 ratio). Only water was used as non-solvent in the case of NMP triblock copolymer solutions.

Nanoprecipitation protocol

To different glass vials placed in a stirring plate and equipped with magnetic bars was added 1.2 mL of non-solvent. To each vial an adequate triblock solution volume (5 % w/w in NMP or

1 % w/w in THF) was added dropwise to reach different solvent/non-solvent ratios (i.e. 0.6 mL for the 1:2 ratio; 0.3 mL for the 1:4 ratio; 0.15 mL for the 1:6 ratio).

In all micellization and nanoprecipitation samples cloudy solutions were obtained. At the end 18 vials containing micellar solutions were obtained. Three of each protocols in the case of NMP samples and six of each protocol in the case of THF (three used water as non-solvent and three ethanol).

Preparation of AFM samples

Self-assembled structures were deposited on silicon wafers by spin-coating of suspension of triblock copolymer in THF/ethanol (or NMP/water). The suspension was spin-coated (SPS Spin 150 spin coater) onto a clean silicon wafer at 1000 rpm for 120 s (or 300 s) with a speed ramp of 100 rpm s^{-1}. The AFM analyses were performed directly on the silicon wafer.

Results and discussion

The amphiphilic ABA triblock copolymer was prepared by a one pot aminolysis/thia-Michael addition involving a *mono*-functional PVDF-Xanthate (PVDF-XA) and a difunctional PEG acrylate (PEGDA) (Scheme 1). The PVDF$_{50}$-XA was synthesized by RAFT polymerization following an already established protocol.[41] The PEG diacrylate (PEGDA) was prepared by simple acrylation of a commercial dihydroxylated PEG (Figure S3). The acrylation reaction resulted in quantitative functionalization of the commercial PEG (Figure S4). Then, the targeted PVDF$_{50}$-*b*-PEG$_{136}$-*b*-PVDF$_{50}$ ABA triblock copolymer was synthesized in relatively high yield (86 %) by coupling reaction using relative stoichiometric equivalents of PVDF and PEG. The conversion of the coupling reaction was followed by ^{1}H NMR and was evidenced by the disappearance of both signals of the xanthate groups at δ = 1.40-1.46 ppm and δ = 4.67-4.77 ppm (conversion of the xanthate end-groups into thiol via aminolysis), and signals of the acrylate groups at δ = 5.85, 6.16 and 6.43 ppm (thia-Michael addition) (Figure S5. The success of the thia-Michael addition was also confirmed by ^{19}F NMR spectroscopy with a up flied shift of the fluorine signals of the –CF$_2$ unit directly bonded to the xanthate moiety from δ = -113.09 to δ = -113.77 ppm (Figure S6). The formation of the triblock copolymers was further confirmed by SEC-HPLC. Figure 1 shows the SEC chromatograms of the two homopolymer precursors and of the resulting ABA triblock. These chromatograms confirm the successful coupling reaction with a clear shift of the triblock copolymer trace towards shorter retention time (higher molar masses). However, a small shoulder at lower retention time reveals the presence of small amounts of residual PVDF precursors that were not removed by precipitation. This residual PVDF is likely the non-functional PVDF-H chains (10 mol %) formed by transfer reactions (estimation made from ^{1}H NMR data (Figure 1), PVDF-H signals at 6.05 – 6.45 ppm). Indeed, the starting PVDF was composed of 90 mol. % of chains terminated by a head-to-head addition (-CH$_2$CF$_2$CF$_2$CH$_2$-XA) and 10 mol. % of chains terminated by a hydrogen atom (-CF$_2$H et -CH$_3$) resulting transfer reaction.
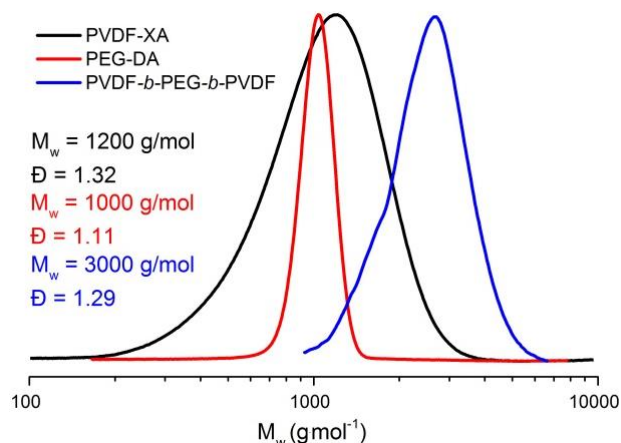
Figure 1. Normalized SEC chromatograms (viscometric detector) of: PVDF-XA (black trace), PEGDA (red trace), PVDF-*b*-PEG-*b*-PVDF (blue trace).

^{1}H diffusion-ordered spectroscopy (DOSY) NMR experiments were also carried out to further characterize the ABA triblock copolymer. These DOSY experiments provide 2D correlation maps showing chemical shifts and diffusion coefficients on the horizontal and vertical axes, respectively.

The ^{1}H DOSY map of the PVDF$_{50}$-*b*-PEG$_{136}$-*b*-PVDF$_{50}$ triblock copolymer (Figure 2 and S7) shows that all ^{1}H NMR signals correlate with a single diffusion coefficient (2.8 10^{-5} m^2 s^{-1}). In comparison DOSY experiments carried out on PVDF-XA and PEGDA provided diffusion coefficients of 9.1 10^{-5} m^2 s^{-1} and 7.5 10^{-5} m^2 s^{-1} respectively These results suggest quantitative coupling reactions without contamination of residual homopolymers.
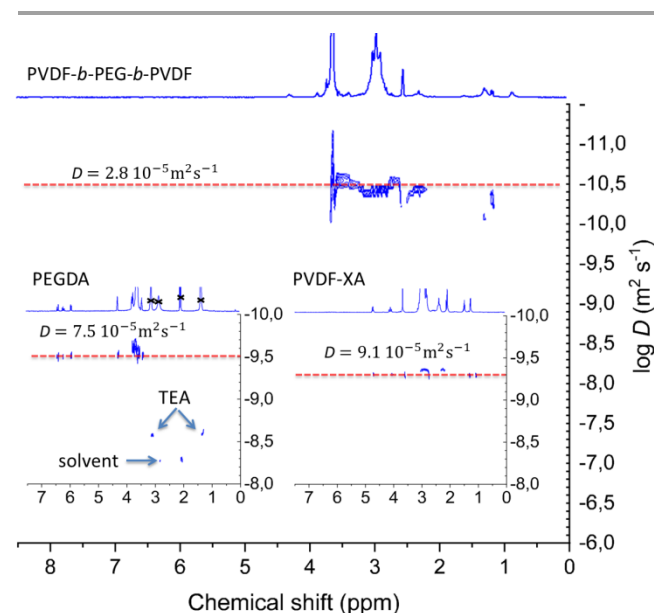

Figure 2. ^{1}H DOSY-NMR spectra of the PVDF-*b*-PEG-*b*-PVDF triblock copolymer (main spectrum), PEGDA (left inset), and PVDF-XA (right inset) recorded in (CD$_3$)$_2$SO at 60 °C. D = diffusion coefficient.

The discrepancy between the SEC and ^{1}H DOSY NMR results are likely due to the higher lower detection limit of ^{1}H DOSY NMR compared to SEC.

Nevertheless these analyses indicate that the protocol used here led to a relatively well defined PVDF-*b*-PEG-*b*-PVDF triblock copolymer (Đ< 1.3).
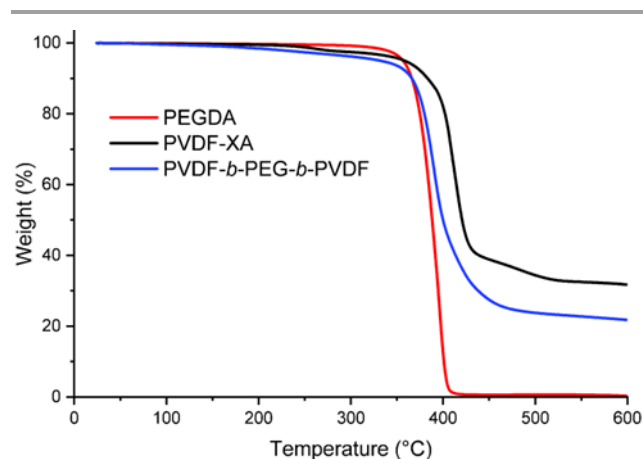

Figure 3. Overlay of the TGA traces the PVDF-xanthate (black trace) and PEG-diacrylate (red trace) precursors, and of the PVDF$_{50}$-*b*-PEG$_{136}$-*b*-PVDF$_{50}$ triblock copolymer (blue trace).

Thermogravimetric analyses (under air) (Figure 3) revealed that the PVDF$_{50}$-*b*-PEG$_{136}$-*b*-PVDF$_{50}$ triblock copolymer displayed a thermal behaviour relatively similar to those of its precursors. No significant weight loss was observed before 348 °C (Td$_{5\%}$ of the triblock) close to the degradation temperature of the PEGDA (Td$_{5\%}$ = 360 °C) , while PVDF-XA started to degrade at marginally higher T (Td$_{5\%}$ = 365 °C, Td$_{10\%}$ = 389 °C). Differential scanning calorimetry (DSC) of the PVDF$_{50}$-*b*-PEG$_{136}$-*b*-PVDF$_{50}$ triblock copolymer revealed the characteristic exothermic and endothermic peaks corresponding to the crystallization and melting transitions at 40.3 and 56 °C for PEG and at 139.5 and 178.3 °C for PVDF, respectively (Figure S13, and Figure 4). These values are in good agreement with those obtained for PEGDA (T$_c$ = 42 °C and T$_m$ = 58 °C) (Figure S12) and PVDF-XA homopolymers (T$_c$ = 140 °C and T$_m$ = 168.7 °C) (Figure. S11). In addition, the DSC thermogram of the triblock (Figure 4 and Figure S13) displayed two distinct glass transition temperatures corresponding to VDF (-34 °C) and PEG (-10 °C), confirming the bulk incompatibility of these two polymers. The DSC thermograms were also used to quantify the degree of crystallinity of the PVDF (47.1%) and of the PEG (53.8%) in the triblock copolymer (See S14 for details on these calculations).

The self-assembly in solution of the new PVDF-based amphiphilic triblock copolymer was then studied.
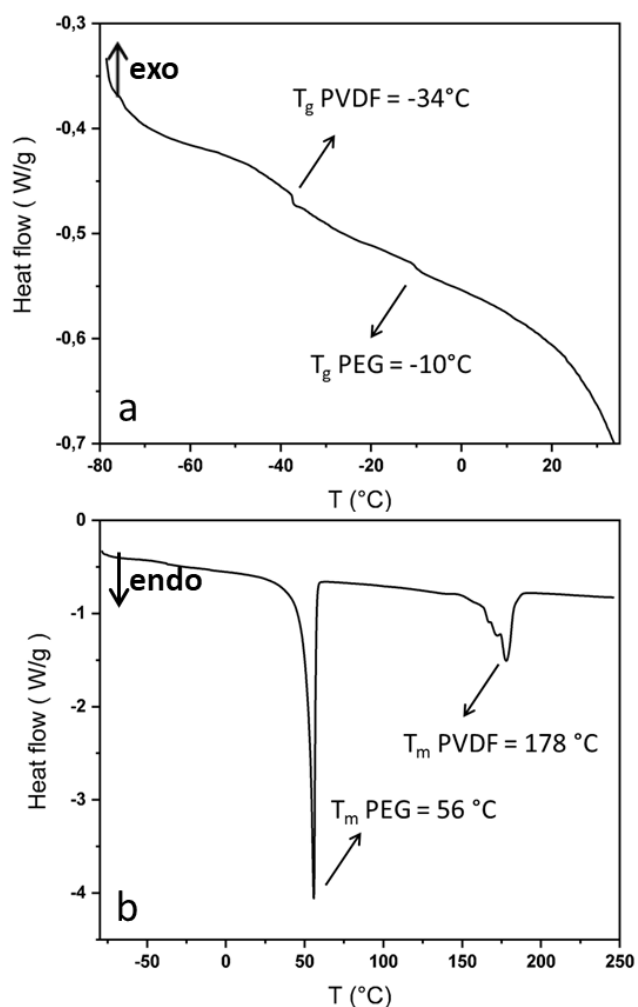
Figure 4. DSC Thermograms of PVDF$_{50}$-b-PEG$_{136}$-b-PVDF$_{50}$ triblock copolymer. a) Area highlighting the glass transitions of PVDF and PEG. b) Area presenting the two endothermic signals corresponding to the melting points of PEG and PVDF.

Among the various methods used to promote the self-assembly of amphiphilic block copolymer in solution, we selected the two most common techniques used so far: (i) Direct dissolution of the polymer in a selective solvent for one of the blocks, and (ii) Dissolution of the block copolymer in a good solvent for both blocks, followed by slow addition of a selective solvent for one of the blocks.[53]

The first method, often called nanoprecipitation, is an easy and direct way to provoke self-assembly and is well-suited for block copolymers with relatively low molar masses and relatively short insoluble block.[53] Given the high hydrophobicity and crystallinity of PVDF, the second method (called here micellization), although more time-consuming, is probably more suitable to the present PVDF-b-PEG-b-PVDF triblock copolymer. Indeed, under nanoprecipitation conditions, self-assembly occurs very fast and generally leads to frozen morphologies. A slower self-assembling process such as the micellization method is more likely to deliver thermodynamically more stable self-assembled structures. Note that due to the non-ergodicity of amphiphilic block

copolymer systems, both methods likely lead to kinetically trapped structures.[54]

Two solutions of the triblock copolymers were prepared: One solution in NMP at 5% w/w, and one solution in THF at 1% w/w. Complete dissolution of the triblock copolymers was achieved only after heating for prolonged time (24 h at 60 °C for THF and at 70 °C for NMP). The molecular dissolution of the triblock was confirmed by DLS (Figure S15). Only 1% w/w solution could be prepared in THF due to the poor solubility of PVDF in THF. The solutions in NMP at 5% w/w and in THF at 1 % w/w were then used to investigate the self-assembly of the triblock copolymer via nanoprecipitation and micellization.

Transmission electron microscopy and atomic force microscopy revealed that the nanoprecipitation protocol led to the formation of small roughly spherical aggregates for the 1:6 NMP: water systems (Figure 5, and S16). These small aggregates with size ranging from 20 to 75 nm displayed relatively rough surfaces and were not perfectly spherical. This is likely caused by the high crystallinity of PVDF and the fast solvent de-mixing times, not leading the BCP to reach kinetically stable morphologies.[44]

When micellar solutions at 1:2 and 1:4 NMP: water ratios were analysed by TEM, only large micrometric aggregates were observed (Figure S16). The concentration of non-solvent was probably not enough at these stages, and the observed non-defined aggregates are due to non-self-assembled BCP.

In the case of the THF: water solvent: non-solvent system, both self-assembly protocols produced vesicles of around 300 nm (Figure 6a, 6b and S16). Higher THF: water ratios led to larger aggregates (Figure S16). As above, better defined particles were obtained at lower solvent: non-solvent ratios.
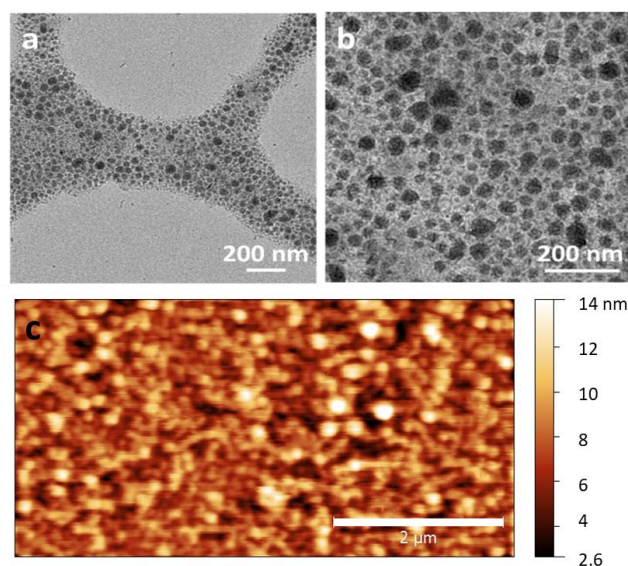

Figure 5. a) and b) TEM images of PVDF$_{50}$-b-PEG$_{136}$-b-PVDF$_{50}$ aggregates obtained from a 5% w/w solution in NMP by nanoprecipitation (NMP:water (1:6)). c) AFM topographic image of these aggregates deposited by spin-coating on a silicon wafer.

In the nanoprecipitation experiments, higher solvent/ non solvent ratios, likely lead to instability of the vesicles and thus, big aggregates of non-assembled polymer are also observed.

In contrast, nanoprecipitation of the THF solution in ethanol using 1:6 (Figure 7b, and S16) lead to the formation of crystalline structures with ovoidal shape and using 1:4 THF: ethanol ratio a mixture of ovoidal, crystalline shard like structures and spheres of various size were observed (Figure 7a, 7c), and S16). Ovoidal crystalline structures have already been reported in our group from PVAc-*b*-PVDF diblock copolymers.[45] In the latter case the corona forming block was not crystalline so the objects observed by TEM should not differ from the ones in solution (i. e. the corona-forming block does not crystallize when the solvent evaporates). Similar structures have been also described by Wang et al. for self-assembled PEG-*b*-PPDO, by Wang J. et al. in the case of a (MPEG)(PCL)(PPE) 3-miktoarm star terpolymer, by Chen et al. for PCL-*b*-PDMAEMA and PCL-*b*-PAA block copolymers and by Rizis et al. for PEG-*b*-PCL. These structures are thought to be formed by crystallisation-driven self-assembly (CDSA).[55–59] The crystallinity of those structures was highlighted by the analysis of the SAED patterns recorded during TEM analysis and compared to the XRD diffraction pattern (Figure 8). From XRD measurement, the two diffraction peaks observed at $2\theta = 19.8$ and 26.5° are found to be characteristic of the PVDF phase. In addition, the specific peak at 26.5° unambiguously evidences the α-crystal phase (no existence of the β- and γ-crystal phases).[60] The XRD pattern also shows two peak at $2\theta = 19.2$ and 23.4° attributed to the crystalline structure of the PEG (see S18).[61]
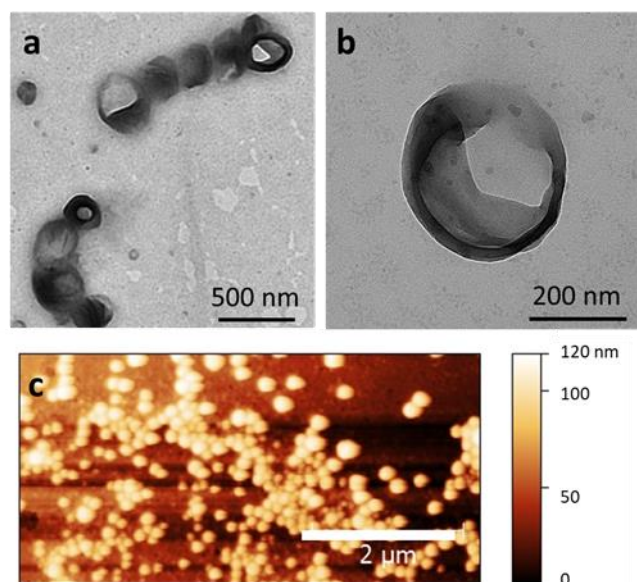

Figure 7. TEM images of PVDF$_{50}$-*b*-PEG$_{136}$-*b*-PVDF$_{50}$ crystalline nanostructures obtained by nanoprecipitation in ethanol of a 1% w/w THF solution in THF; a) and c): THF: ethanol = 1:4; b): THF: ethanol = 1:6. d) schematic representation of the objects observed in a) and c).

Figure 8. XRD pattern of PVDF$_{50}$-*b*-PEG$_{136}$-*b*-PVDF$_{50}$ recorded at room temperature. Red dots and blue rhombus are PVDF and PEG characteristic diffractions. The inset is the SAED pattern of the objects observed in Figure 7b and 7c obtained during TEM analysis (* correspond to the Bragg spots observed). Note: Attempts to record SAED patterns on the other self-assembled morphologies presented in this paper failed due to rapid amorphisation of the structures under the elecron beam.

Figure 6. TEM images of PVDF$_{50}$-*b*-PEG$_{136}$-*b*-PVDF$_{50}$ aggregates obtained from: a) and b) 1% w/w solution in THF by micellization (THF: ethanol (1:6)). c) AFM topographic image of these aggregates deposited by spin-coating on a silicon wafer.
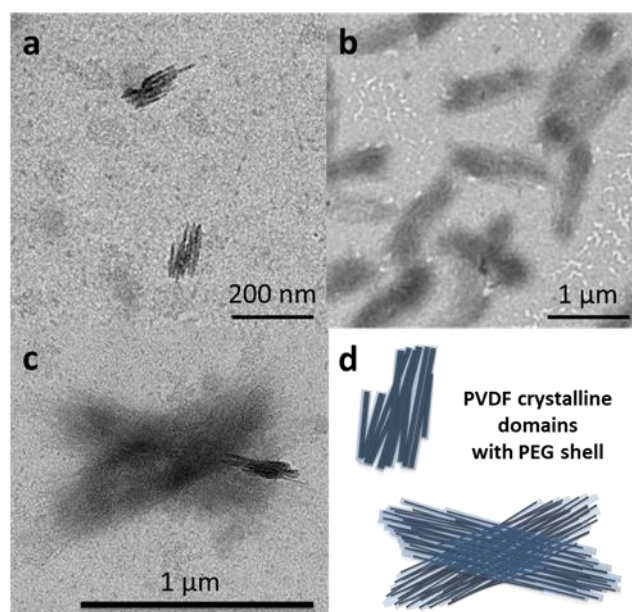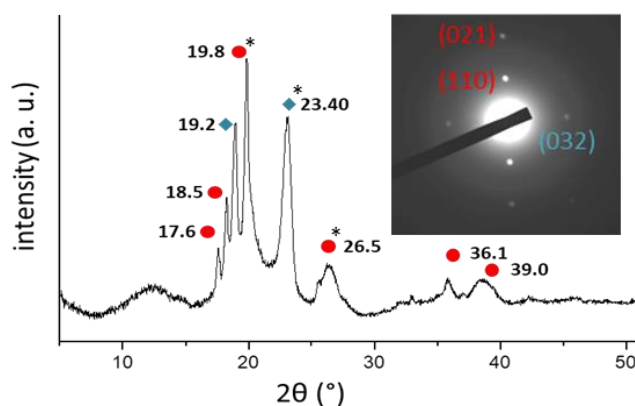
Moreover, the symmetrical Bragg spots of (110)$_{PVDF}$ and (021)$_{PVDF}$ can be clearly observed from the SAED pattern, indicating that the ovoidal structures may be considered to be single crystals of PVDF (the entire object analysed was inside the selected area). In addition, the symmetrical spots of (032)$_{PEG}$ indicate that the PEG is crystalline too. According to previous reports preparation of single-crystals is complicated and time-consuming (self-seeding method) and it has never been reported for PVDF-based block copolymers.[59]

Conclusions

An ABA PVDF-*b*-PEG-*b*-PVDF amphiphilic triblock copolymer was synthesized using an efficient one-pot aminolysis / thia-Michael addition of a PVDF prepared by RAFT and PEG diacrylate. This novel PVDF-based ABA triblock copolymer was thoroughly characterised by ^{1}H, ^{1}H DOSY and ^{19}F-NMR spectroscopies, GPC as well as TGA, DSC and XRD. These characterizations proved the coupling strategy efficient and revealed a relatively well-defined (low Đ) triblock copolymer. As expected, the triblock copolymer had thermal resistance close to that of PEG and inferior to that of PVDF and both blocks present the inherent crystallinity of these materials. The self-assembly of this amphiphilic triblock copolymer was performed using nanoprecipitation and micellization protocols using NMP or THF as good solvents and water or ethanol as the block selective solvents. In most cases, the self-assembly experiments led to roughly spherical aggregates with size ranging from 20 to 75 nm and vesicles up to 300 nm. However, when THF solutions were used under nanoprecipitation protocols in ethanol, micrometric crystalline oval morphologies were obtained. The crystallinity of both α-PVDF and PEG in those structures was confirmed by SAED patterns recorded during TEM analysis and identified by XRD measurement. These original triblock copolymers and self-assembled morphologies may offer new opportunities to design electroactive structures at the nano- and micrometric scales.

Conflicts of interest

There are no conflicts to declare.

Acknowledgements

Notes and references

1   A.-C. Genix, G. P. Baeza and J. Oberdisse, *Eur. Polym. J.*, 2016, **85**, 605–619.

2   J. Herzberger, K. Niederer, H. Pohlit, J. Seiwert, M. Worn, F. R. Wurm and F. Holger, *Chem. Rev.*, 2016, **116**, 2170–2243.

3   V. Abetz, I. Polymerforschung and G. G. Gmbh, *Adv. Polym. Sci.*, 2005, **189**, 125–212.

4   S. Mai, W. Mingvanish, S. C. Turner, C. Chaibundit, J. P. A. Fairclough, F. Heatley, M. W. Matsen, A. J. Ryan and C. Booth, *Macromolecules*, 2000, **33**, 5124–5130.

5   M. W. Matsen, *Macromolecules*, 2012, 2161–2165.

6   A. M. Mayes, M. Olvera, D. Cruz, A. M. Mayes, M. Olvera and D. Cruz, *J. Chem. Phys.*, 1989, **91**, 7228–7235.

7   G. Lopez, M. Guerre, J. Schmidt, Y. Talmon, V. Ladmiral, J.-P. Habas and B. Améduri, *Polym. Chem.*, 2016, **7**, 402–409.

8   A. Ding, G. Lu, H. Guo and X. Huang, *Polym. Chem.*, 2017, **8**, 6997–7008.

9   S. Nehache, M. Semsarilar, M. In, P. Dieudonné-George, J. Lai-Kee-Him, P. Bron, D. Bouyer, A. Deratani and D. Quemener, *Polym. Chem.*, 2017, **8**, 3357–3363.

10   P. He, X. Li, M. Deng and H. Liang, *Soft Matter*, 2010, **6**, 1539–1546.

11   G. Riess, *Prog. Polym. Sci.*, 2003, **28**, 1107–1170.

12   T. Zinn, L. Willner, K. D. Knudsen and R. Lund, *Macromolecules*, 2017, **50**, 7321–7332.

13   S. Jain and F. S. Bates, *Macromolecules*, 2004, **37**, 1511–1523.

14   P. Bhargava, J. X. Zheng, P. Li, R. P. Quirk, F. W. Harris and S. Z. D. Cheng, *Macromolecules*, 2006, **39**, 4880–4888.

15   T. Annable, R. Buscall, R. Ettelaie and D. Whittlestone, *J. Rheol.*, 1993, **37**, 695–726.

16   E. Villar-Alvarez, E. Figueroa-Ochoa, S. Barbosa, J. F. A. Soltero, P. Taboada and V. Mosquera, *RSC Adv.*, 2015, **5**, 52105–52120.

17   A. Cambon, E. Figueroa-Ochoa, M. Blanco, S. Barbosa, J. F. A. Soltero, P. Taboada and V. Mosquera, *RSC Adv.*, 2014, **4**, 60484–60496.

18   I. Park, S. Park, D. Cho, T. Chang, K. Lee and Y. J. Kim, *Macromolecules*, 2003, **36**, 8539–8543.

19   D. J. Keddie, *Chem. Soc. Rev.*, 2014, **43**, 496–505.

20   J. Jennings, M. Beija, J. T. Kennon, H. Willcock, R. K. O'Reilly, S. Rimmer and S. M. Howdle, *Macromolecules*, 2013, **46**, 6843–6851.

21   K. Matyjaszewski, *Macromolecules*, 2012, **45**, 4015–4039.

22   N. V. Tsarevsky, P. McCarthy, W. Jakubowski, J. Spanswick and K. Matyjaszewski, *Tech. Proc. 2008 NSTI Nanotechnol. Conf. Trade Show, NSTI-Nanotech, Nanotechnol. 2008*, 2008, **2**, 665–668.

23   C.-H. Peng, T.-Y. Yang, Y. Zhao and X. Fu, *Org. Biomol. Chem.*, 2014, **12**, 8580–8587.

24   P. Mandal, S. Choudhury and N. K. Singha, *Polym.*, 2014, **55**, 5576–5583.

25   Z. Xue, Z. Wang, D. He, X. Zhou and X. Xie, *J. Polym. Sci.*

Part A Polym. Chem., 2016, **54**, 611–620.

26 D. A. Shipp, Q. Lou, J. G. Linhardt and F. K. Jay, *Polym. Chem.*, 2017, **55**, 3387–3394.

27 B. A. Riga, M. D. Neves, A. E. H. Machado, D. M. S. Araújo, J. R. Souza, O. R. Nascimento, V. T. Santana, C. C. S. Cavalheiro, V. P. Carvalho-Jr and B. E. Goi, *Inorganica Chim. Acta*, 2018, **471**, 620–629.

28 J. Demarteau, B. Améduri, V. Ladmiral, M. A. Mees, R. Hoogenboom, A. Debuigne and C. Detrembleur, *Macromolecules*, 2017, **50**, 3750–3760.

29 A. Kermagoret, N. D. Q. Chau, B. Grignard, D. Cordella, A. Debuigne, C. Jérôme and C. Detrembleur, *Macromol. Rapid Commun.*, 2016, **37**, 539–544.

30 R. Fuhrer, I. K. Herrmann, E. K. Athanassiou, R. N. Grass and W. J. Stark, *Langmuir*, 2011, **27**, 1924–9.

31 B. M. Ameduri, R. Poli, V. Ladmiral, S. Banerjee, A. Debuigne and C. Detrembleur, *Angew. Chemie Int. Ed.*, 2018, **57**, 2934–2937.

32 Y. Li, T. Soulestin, V. Ladmiral, B. Ameduri, T. Lannuzel, F. Domingues Dos Santos, Z. M. Li, G. J. Zhong and L. Zhu, *Macromolecules*, 2017, **50**, 7646–7656.

33 T. Soulestin, P. Marcelino Dos Santos Filho, V. Ladmiral, T. Lannuzel, F. Domingues Dos Santos and B. Améduri, *Polym. Chem.*, 2017, **8**, 1017–1027.

34 T. Soulestin, V. Ladmiral, F. Domingues, D. Santos and B. Améduri, *Prog. Polym. Sci.*, 2017, **72**, 16–60.

35 T. Soulestin, V. Ladmiral, F. Domingues, D. Santos and B. Améduri, *Prog. Polym. Sci.*, 2017, **72**, 16–60.

36 M. Guerre, S. M. W. Rahaman, B. Ame, R. Poli, V. Ladmiral and I. C. Gerhardt, *Macromolecules*, 2016, **49**, 5386–5396.

37 R. Guerre, Marc; Wahidur Rahaman, S. M.; Améduri, Bruno; Poli and V. Ladmiral, *Polym. Chem.*, 2016, **7**, 6918–6933.

38 M. Guerre, M. Uchiyama, E. Folgado, M. Semsarilar, B. Améduri, K. Satoh, M. Kamigaito and V. Ladmiral, *ACS Macro Lett.*, 2017, **6**, 393–398.

39 Y. Wu, L. Chen, X. Sun, J. Xu, G. Gu and J. Qian, *J. Saudi Chem. Soc.*, 2017, **21**, 713–719.

40 Y. Patil, P. Bilalis, G. Polymeropoulos, S. Almahdali, N. Hadjichristidis and V. Rodionov, *Mol. Pharm.*, 2018, **15**, 3005–3009.

41 M. Guerre, B. Campagne, O. Gimello, K. Parra, B. Ameduri and V. Ladmiral, *Macromolecules*, 2015, **48**, 7810–7822.

42 V. Ladmiral, *Polym. Chem.*, 2016, **7**, 6918–6933.

43 M. Guerre, J. Schmidt, Y. Talmon, B. Améduri and V. Ladmiral, *Polym. Chem.*, 2017, **8**, 1125–1128.

44 M. Guerre, M. Semsarilar, C. Totée and G. Silly, *Polym. Chem.*, 2017, **8**, 5203–5211.

45 M. Guerre, M. Semsarilar, F. Godiard, B. Améduri and V. Ladmiral, *Polym. Chem.*, 2017, **8**, 1477–1487.

46 L. Li, J. Li and S. Zheng, *Polymer*, 2018, **142**, 61–71.

47 M. Sommer, H. Komber, S. Huettner, R. Mulherin, P. Kohn, N. C. Greenham and W. T. S. Huck, *Macromolecules*, 2012, 4142–4151.

48 V. Ladmiral, M. Semsarilar, I. Canton and S. P. Armes, *J. Am. Chem. Soc.*, 2013, **135**, 13574–13581.

49 V. Ladmiral, A. Charlot, M. Semsarilar and S. P. Armes, *Polym. Chem.*, 2015, **6**, 1805–1816.

50 M. Guerre, B. Ameduri and V. Ladmiral, *Polym. Chem.*, 2016, **7**, 441–450.

51 J. R. Mckee, V. Ladmiral, J. Niskanen, H. Tenhu and S. P. Armes, *Macromolecules*, 2011, **44**, 7692–7703.

52 X. Liu, O. Coutelier, S. Harrisson, T. Tassaing, J. Marty and M. Destarac, *ACS Macro Lett.*, 2015, **4**, 89–93.

53 M. Karayianni and S. Pispas, *Self-Assembly of Amphiphilic Block Copolymers in Selective Solvents*, 2016.

54 R. C. Hayward and D. J. Pochan, *Macromolecules*, 2010, **43**, 3577–3584.

55 H. Wang, C.-L. Liu, G. Wu, S.-C. Chen, F. Song and Y.-Z. Wang, *Soft Matter*, 2013, **9**, 8712–8722.

56 Y. Yuan and J. Wang, *Colloids Surfaces B Biointerfaces*, 2011, **85**, 81–85.

57 J. Wang, W. Zhu, B. Peng and Y. Chen, *Polymer.*, 2013, **54**, 6760–6767.

58 J. Wang, Y. Lu and Y. Chen, *Polymer).*, 2019, **160**, 196–203.

59 G. Rizis, T. G. M. Van De Ven and A. Eisenberg, *Angew. Chemie - Int. Ed.*, 2014, **53**, 9000–9003.

60 P. Martins, A. C. Lopes and S. Lanceros-Mendez, *Prog. Polym. Sci.*, 2014, **39**, 683–706.

61 W. A. K. Mahmood, M. H. Azarian, W. F. bt Wan Fathilah and E. Kwok, *J. Appl. Polym. Sci.*, 2017, **134**, 1–9.